



Marcin Godzierz*, Anita Olszówka-Myalska

Silesian University of Technology, Department of Materials Science and Metallurgy, Institute of Materials Science, ul. Krasińskiego 8, 40-019 Katowice, Poland

**Corresponding author. E-mail: marcin.godzierz@polsl.pl*

Received (Otrzymano) 5.08.2018

MICROSTRUCTURAL CORROSION EFFECTS ON CARBON FOAM-AZ31 MAGNESIUM MATRIX COMPOSITE SURFACE

In the article, a new composite was studied as a potential biomaterial. The effects of the interaction of distilled water with the polished surface of an AZ31 magnesium matrix composite reinforced with open-celled glassy carbon foam fabricated by the pressure infiltration method were investigated. The experiment was conducted in the time range of 1 minute - 4 hours and the microstructure was examined by scanning electron microscopy. In the initial unetched material, at the glassy carbon-metal interface, a zone of needle-like phases was detected. After a 1÷10 minute interaction with the water, disintegration of that zone was revealed and that type of material degradation proceeded deeper into the composite as the time increased. Another type of corrosion was observed in microareas of the magnesium alloy matrix, but only after approx. 1 hour when corrosion pits were recorded. The results of X-ray mapping showed an increase in the oxygen concentration in both types of corrosion products, but the reason for the corrosion in the region between the carbon foam and the AZ31 matrix is degradation of the hydrophilic aluminium based carbide phases, while in the composite matrix, typical electrochemical corrosion of magnesium occurred.

Keywords: magnesium matrix composite, carbon open-celled foam, corrosion, interface, biomaterials

MIKROSTRUKTURALNE EFEKTY KOROZJI NA POWIERZCHNI KOMPOZYTU PIANA WĘGLOWA-OSNOWA MAGNEZOWA AZ31

Odporność korozyjna magnezu i jego stopów, w tym AZ31 w środowisku wodnym jest słaba i materiały te stosowane są na bioresorbowalne implanty. Wprowadzenie do magnezu otwartokomórkowych pian węglowych pozwala uzyskać materiał zawierający dwa biozgodne komponenty o różnej odporności korozyjnej i tym samym kompozyt ulegający selektywnej korozji. Potencjalnie powinno to ułatwić wrastanie tkanek pomiędzy węglowy szkielet, który znacznie później sam ulegnie resorpcji. W pracy przedstawiono wyniki badań wstępnych oddziaływania wody destylowanej na mikrostrukturę kompozytu z osnową ze stopu AZ31, zawierającego otwartokomórkową pianę węglową (C_{of}) firmy Duocel 100 ppi o porowatości 97%, charakteryzującą się wstęgową budową ścian (RVC). Kompozyt wytworzono metodą infiltracji ciśnieniowej w atmosferze próżni, zgodnie z autorską procedurą. Metodą SEM z EDS charakteryzowano mikrostrukturę wypolerowanej powierzchni kompozytu w stanie wyjściowym i poddanej oddziaływaniu wody destylowanej w czasie od 1 minuty do 4 godzin. Wykazano występowanie dwóch mechanizmów degradacji mikrostruktury wynikających z oddziaływania wody destylowanej z kompozytem. Jeden, charakterystyczny dla stopów magnezu, wystąpił po 1 godzinie ekspozycji. Polegał on na powstawaniu na mikroobszarach osnowy niewielkich początkowo narostów produktów korozji, które z czasem całkowicie pokryły stop magnezu. Drugi obserwowany efekt oddziaływania dotyczył strefy połączenia metal-węgiel szklisty i ujawnił się po bardzo krótkim czasie. Występujące na granicy rozdziału iglaste fazy, zidentyfikowane pośrednio jako węglkowe zawierające aluminium, ulegały postępującej destrukcji. Proces był widoczny w przedziale czasu 1 do 10 minut, po którym dalszych zmian na powierzchni nie obserwowano. Wykazały je dopiero obserwacje przekroju poprzecznego, wskazujące na postępowanie procesu degradacji w głąb materiału. Uzyskane wyniki potwierdziły selektywną korozję kompozytu, ale aplikacja stopu AZ31 wywołuje na granicy emisję produktów gazowych, co wskazuje na celowość użycia w charakterze osnowy innego stopu magnezu.

Słowa kluczowe: kompozyty magnezowe, otwartokomórkowe piany węglowe, korozja, granica rozdziału, biomateriały

INTRODUCTION - AIM OF RESEARCH

Magnesium matrix composites can be reinforced with ceramic components of different phase compositions, shapes and sizes. In the literature, in the group of carbon materials used as reinforcement, fiber preforms, short carbon fibers, carbon nanotubes and particles of graphite or glassy carbons are proposed [1-9]. In the carbon-magnesium system, the basic bonding that is

formed in consolidation processes is of the oxide type, due to the presence of oxygen absorbed by the carbon component. That induces the formation of an MgO nanolayer at the interface, and doping of the magnesium matrix by the alloying elements causes additional oxide and carbide phases to form in the interface region. Moreover, in the case of liquid phase processes,

agglomeration of intermetallic phases, characteristic of a magnesium alloy composition, occurred as a result of microsegregation processes connected with metal crystallization [8-12]. Current research works focusing on metal matrix composites present the application of open-celled foams instead of microsized fibers or particles, owing to the possibility of a perfect reinforcement distribution design, without the macro and microsegregation effects [8, 9, 13-17] characteristic of different manufacturing methods such as stir casting, centrifugal casting or fiber preform infiltration [10-20].

The magnesium matrix composite reinforced with carbon open-celled foams (C_{of}) is located in this field of new material research. The processing of that composite requires consideration of both the technical aspects of magnesium technologies, such as high oxidation intensity, and problems characteristic of component consolidation, such as effective penetration of the carbon foam by the metal matrix. In work [19], we proposed a two-step technology consisting in pure magnesium powder compaction in C_{of} cells by the vibration method and then hot pressing in vacuum. In the presented work, another method was applied in composite processing, i.e. pressure infiltration [20], and instead of pure magnesium, a commonly used magnesium alloy of good castability, AZ31, was used.

The purpose of the study was to examine the structural effects in the composite induced on the material surface by distilled water so as to ascertain its potential application as a biomaterial. Magnesium and its alloys, such as AZ31, are well-known in the literature as materials for biodegradable implants [21-28], while carbon materials are considered biocompatible [29-30]. Therefore, it can be expected that a magnesium based composite with open-celled carbon foam will demonstrate selective corrosion [31, 32] and the new biological tissue will replace the magnesium in the implants, while the carbon component structure will aid tissue growth until later foam absorption.

MATERIALS AND METHODS

The composite was fabricated from the AZ31 alloy, of the composition presented in Table 1 and a carbon open-celled foam 100 ppi, manufactured by the Duocel company, denoted as C_{of} . The macrostructure and microstructure are shown in Figure 1. The applied C_{of} of 97% porosity consists of regular cells with windows facilitating liquid metal transport and characteristic band-like shaped walls, and that foam is also called reticulated vitreous carbon (RVC) in the literature. The process of component consolidation was conducted according to patented procedure [20] in vacuum atmosphere at the temperature of 690°C for 5 minutes with the maximal pressure of 5 MPa. The application of additional pressure was necessary because our earlier examinations of carbon foams and liquid magnesium as well as some magnesium alloys [33] showed ineffectiveness of the self-infiltration technique for component

consolidation, and that was in good agreement with the literature data reporting poor wettability of carbon materials by magnesium [33-35].

TABLE 1. Chemical composition of AZ31 alloy [wt.%] [21, 25]
TABELA 1. Skład chemiczny stopu AZ31 [% masowej] [21, 25]

Element	Al	Zn	Mn	Mg
[wt.%]	2.5÷3.5	0.7÷1.3	0.20	rest

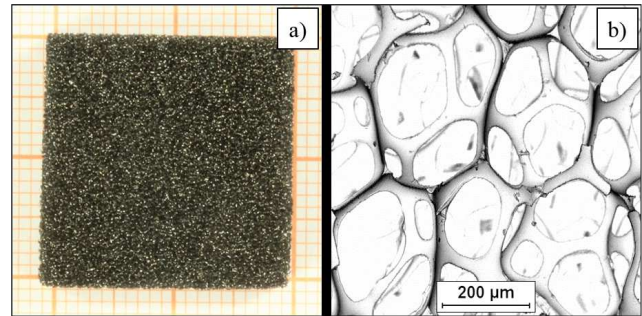


Fig. 1. Macrograph (a) and SEM micrograph (b) of 100 ppi open-celled carbon foam, fabricated by Duocel company

Rys. 1. Makrofotografia (a) i mikrografia SEM (b) otwarto-komórkowej piany węglowej 100 ppi produkcji firmy Duocel

From the C_{of} -AZ31 composite a cuboidal sample of the dimensions 10x5x5 mm was cut out, then grounded and polished in a non-water environment and examined by scanning electron microscopy. For microstructure characterization, a Hitachi S4200 microscope with an EDS spectrometer was applied.

The character of the occurring corrosion processes was analyzed after immersing the composite sample in distilled water at the temperature of 20°C for 4 hours. The microstructure of the sample was checked after 1, 5, and 10 minutes, and then after 1, and 4 hours. After the set exposure time in the water, the sample was immersed in alcohol and then dried in an air stream.

In the microstructure examination, the secondary electron mode (SE) and EDS analysis were applied, and the results were recorded for the same microareas of the composite sample, just after polishing and after each water immersion time. That procedure enables direct control of the composite microstructure evolution induced by interaction with the water. Finally, after 4 hours of water interaction, a sample was cut out, yet this time, perpendicular to the previously polished and then immersed surface and then prepared by grinding and polishing in a non-water environment for the light microscope observation (Nikon Eclipse MA-200). The reason for that examination procedure was to reveal the depth of the corrosion effects recorded earlier at the composite material surface.

RESULTS AND DISCUSSION

The results of the microstructure examination by SEM with EDS are shown in Figures 2-7. The observations of the composite microstructure just after pressure

infiltration presented in Figures 2 and 3 revealed C_{of} well filled by the AZ31 alloy and continuous bonding between the components with the absence of noticeable micropores. However, they also revealed two characteristic effects: a zone of needle-like phases was formed at the interface and microdestruction of mainly the carbon foam edges occurred. The EDS mapping results obtained both at lower (250x, Fig. 2) and higher (2000x, Fig. 3) magnification revealed the presence of aluminium and probably magnesium, as well as the absence of zinc and manganese in the areas with needle-like phases. In that system, the presence of intermetallic phases typical of the AZ31 magnesium e.g. Al12Mg17 alloy, could not be excluded, because they can crystallize in the interface region during composite processing [36, 37]. Nonetheless, they can be too fine to be detected by the EDS resolution and their presence can be confirmed only by several diffraction patterns (SADP) in transmission electron microscopy (TEM). The signal of oxygen's characteristic radiation was not recorded in the interface zone either, but that is understandable because of the nanometric thickness of the oxide layers characteristic of magnesium matrix composites [4, 37].

The needle-like morphology of the phases observed in the interface region and their absence in the other matrix region, as well as destruction of the glassy carbon foam surface during component consolidation suggest the presence of a carbide phase. That effect is known in the literature [37] and it is a consequence of a negative value of Gibbs free energy for the reaction $4Al + 3C \rightarrow Al_4C_3$, where $\Delta G = -167.005$ kJ (determined by the Chemistry 4.1 programme) at the temperature of composite consolidation. The resolution of the EDS method does not make it possible to clearly confirm or exclude the presence of Mg in the needle-like phase, but based on literature data [37], formation of the $MgAl_2C_2$ carbide in that area is also highly probable. Because both carbides containing aluminium are hydrophilic, their destruction in the water environment, as well as the formation of aluminium hydroxide and methane, will confirm their presence according to reactions (1) and (2):

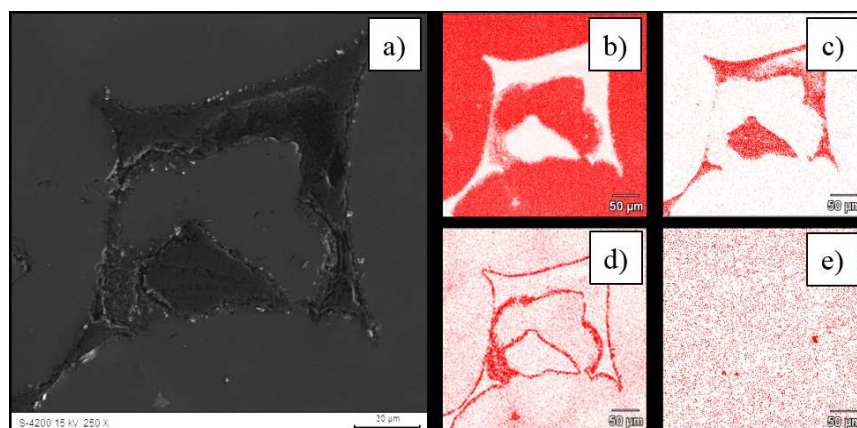


Fig. 2. SEM micrograph of as manufactured C_{of} - AZ31 composite surface (a) and X-ray elemental mapping of: magnesium (b), carbon (c), aluminium (d) and oxygen (e)

Rys. 2. Mikrofotografia SEM powierzchni kompozytu C_{of} - AZ31 w stanie wyjściowym (a) i mapping promieniowania X pierwiastków: magnezu (b), węgla (c), aluminium (d) i tlenu (e)

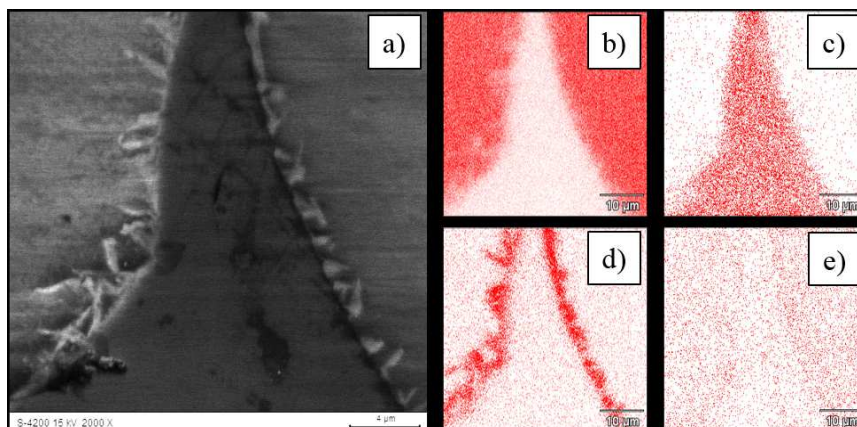


Fig. 3. SEM micrograph of as manufactured C_{of} - AZ31 composite surface, needle-like phases visible in interface region (a) and X-ray elemental mapping of: magnesium (b), carbon (c), aluminium (d) and oxygen (e)

Rys. 3. Mikrofotografia SEM powierzchni kompozytu C_{of} - AZ31 w stanie wyjściowym, na granicy rozdziálu widoczne fazy iglaste (a) i mapping promieniowania X pierwiastków: magnezu (b), węgla (c), aluminium (d) i tlenu (e)

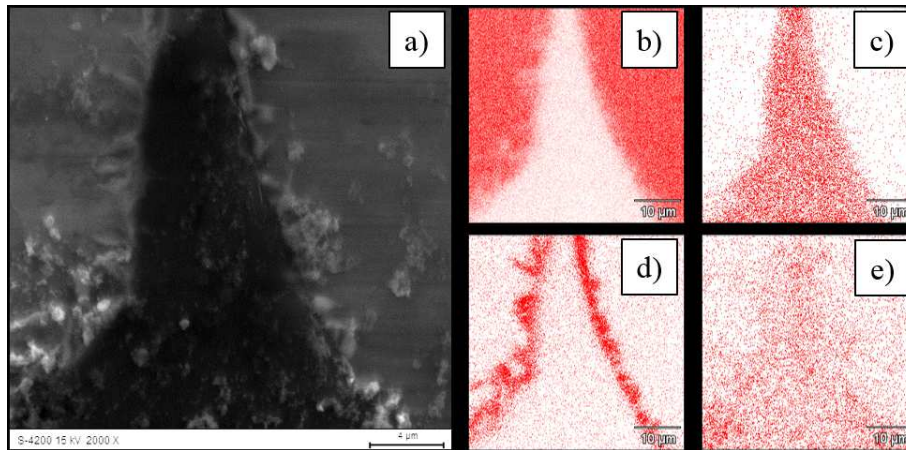


Fig. 4. SEM micrograph of C_{of} - AZ31 composite surface after immersion in distilled water for 1 min (a) and X-ray elemental mapping of: magnesium (b), carbon (c), aluminium (d) and oxygen (e)

Rys. 4. Mikrofotografia SEM powierzchni kompozytu C_{of} - AZ31 po zanurzeniu w wodzie destylowanej przez 1 minutę (a) i mapping promieniowania X pierwiastków: magnezu (b), węgla (c), aluminium (d) i tlenu (e)

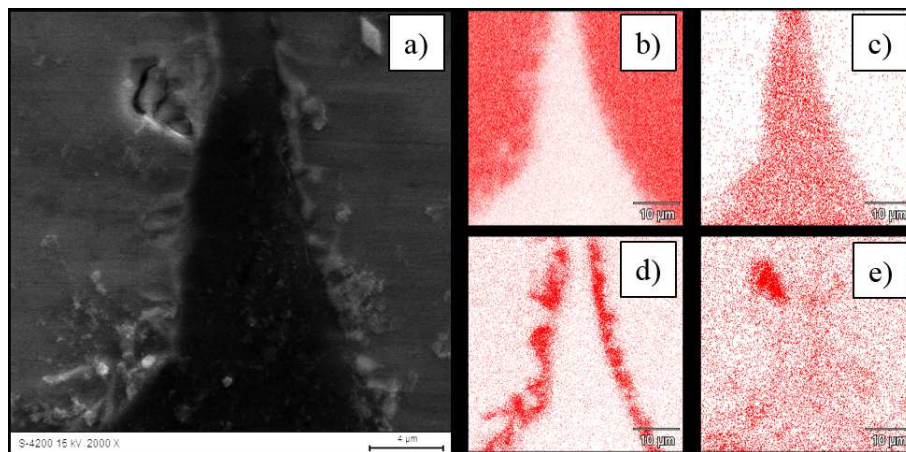


Fig. 5. SEM micrograph of C_{of} - AZ31 composite surface after immersion in distilled water for 5 min (a) and X-ray elemental mapping of: magnesium (b), carbon (c), aluminium (d) and oxygen (e)

Rys. 5. Mikrofotografia SEM powierzchni kompozytu C_{of} - AZ31 po zanurzeniu w wodzie destylowanej przez 5 minut (a) i mapping promieniowania X pierwiastków: magnezu (b), węgla (c), aluminium (d) i tlenu (e)

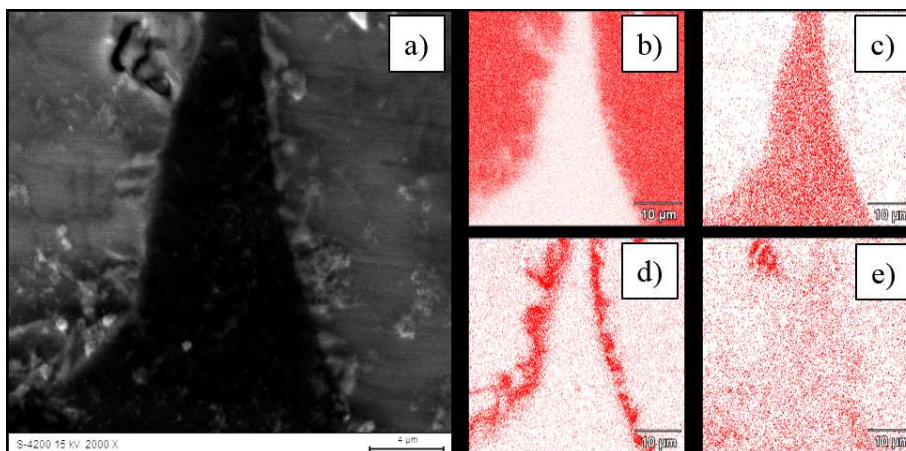


Fig. 6. SEM micrograph of C_{of} - AZ31 composite surface after immersion in distilled water for 10 min (a) and X-ray elemental mapping of: magnesium (b), carbon (c), aluminium (d) and oxygen (e)

Rys. 6. Mikrofotografia SEM powierzchni kompozytu C_{of} - AZ31 po zanurzeniu w wodzie destylowanej przez 10 minut (a) i mapping promieniowania X pierwiastków: magnezu (b), węgla (c), aluminium (d) i tlenu (e)

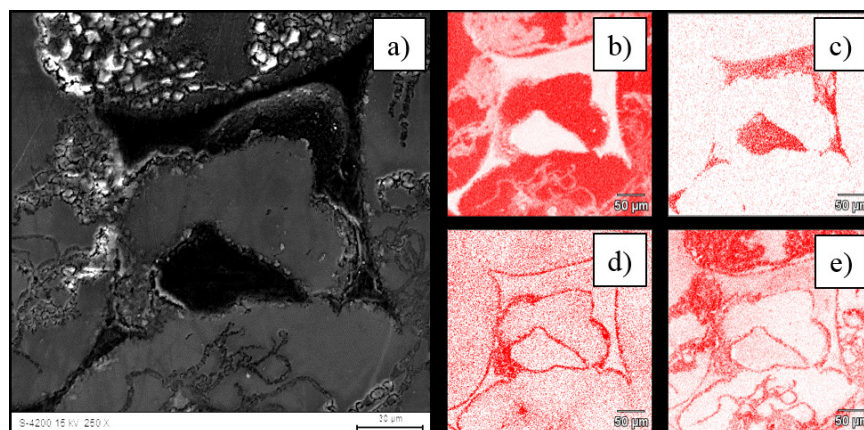


Fig. 7. SEM micrograph of C_{of} - AZ31 composite surface after immersion in distilled water for 1 h (a) and X-ray elemental mapping of: magnesium (b), carbon (c), aluminium (d) and oxygen (e)

Rys. 7. Mikrofotografia SEM powierzchni kompozytu C_{of} - AZ31 po zanurzeniu w wodzie destylowanej przez 1 godzinę (a) i mapping promieniowania X pierwiastków: magnezu (b), węgla (c), aluminium (d) i tlenu (e)

The first changes in the C_{of} - AZ31 composite microstructure on the polished surface were noticed in the SEM micrographs after 1 minute of exposure to the distilled water (Fig. 4), but at the interface only. Minor degradation processes of the needle-like phase occurred and the formation of a new product was visible. In that region, EDS mapping, except for aluminium, reveals the presence of oxygen and it suggests hydroxide formation (Fig. 4e). Despite the microstructure evolution effect, the needle-like phases were still locally visible and it was characteristic that the growth of a new phase occurred over the polished surface. Additionally, the immersion tests of the composite were accompanied by the emission of gas smelling like methane.

Extending the exposure time in the water to 5 minutes induced (Fig. 5) microstructure changes similar to the ones observed earlier, and the increase in the characteristic radiation intensity of oxygen was measured through X-ray mapping (Fig. 5d). A further increase in the contact time of the composite with the water to 10 minutes (Fig. 6) caused changes in the shape of the observed phases without a significant increase in the X-ray radiation intensity of oxygen. It suggests the effect of hydroxide rinsing from the composite surface after subsequent sample immersion. Moreover, two issues must be mentioned. In the time range of 1-10 minutes, no corrosion effects were observed in the microareas of the AZ31 magnesium matrix, but some destruction at the C_{of} surface was detected. The reason for that second phenomenon is the diffusive mechanism of the growth of aluminium containing needle-like carbides, which occurs mainly in the matrix, but also in the carbon material.

When the time of composite immersion was increased to 1 and 4 hours, observation of the composite surface by SEM did not reveal any evolution of the C_{of} - AZ31 interface microstructure, and one may expect that all the hydrophilic phases had reacted with the water. However, after 1 hour, corrosion effects in the AZ31 matrix were evident, which is confirmed

when we compare Figures 2 and 7. In the corroded sample, besides degradation of the interface region, new light irregular phases are visible in SEM, and the EDS results show a high oxygen content with a decrease in the magnesium concentration, which suggests the formation of magnesium oxide or magnesium hydroxide. An increase in the experiment time to 4 hours entailed the growth of corrosion products and finally the effect of the metallic microareas being coated by new phases. Such changes in the AZ31 microstructure induced by corrosion in water are known and described in the literature [21-23, 25].

The question that arises based on the microstructure changes observed at the composite surface is how deep their reach into the as-manufactured material is, and that problem is illustrated by Figure 8, which shows a cross section of the sample after a 4 hour test.

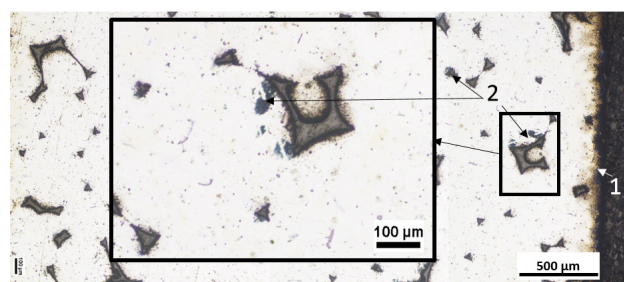


Fig. 8. LM micrograph of C_{of} - AZ31 composite, cross section after immersion in distilled water for 4 h, 1 - surface exposed to water, 2 - corrosion effects around carbon foam

Rys. 8. Mikrofotografia LM przekroju poprzecznego kompozytu C_{of} - AZ31 po zanurzeniu przez 4 h w wodzie destylowanej, 1 - powierzchnia kontaktu, 2 - zmiany korozyjne wokół piany węglowej

The effect of microstructure degradation at the C_{of} - AZ31 interface is observed up to 1000 μm in the composite depth and that exhibits the role of the carbon component geometry in the material degradation. A continuous foam facilitates access of the water to the inside of the composite, similar to the continuous car-

bon fiber preforms, but in contrast to dispersed reinforcing phases, such as short carbon fibers and glassy carbon particles. This process is similar to corrosion along the grain boundaries, well known in metallic materials. In the case of the AZ31 microareas in the examined composite, the layer of corrosion products formed at the surface was uniform and less than 100 μm , which means one order of magnitude less.

In further research, potentiostatic measurements will be performed for precious kinetic characterization of the corrosion processes as well for different magnesium matrix compositions, with the purpose to study the influence of magnesium alloying elements on the degradation mechanism of composites with glassy carbon foams.

CONCLUSIONS

1. During manufacturing performed by pressure infiltration of a new composite material consisting of open-celled carbon foam (C_{of}) and an AZ31 magnesium alloy matrix, both proper foam penetration and proper carbon wetting by the liquid metal were ensured.
2. The applied process parameters induced, on the microscale, damage of the carbon foam surface as well as formation of needle-like phases containing aluminium, which suggests the formation of an aluminium based carbide phase at the interface. Microstructure changes of the C_{of} - AZ31 composite caused by contact with distilled water in the time range of 1 minute - 4 hours were observed, irrespective of the applied time of exposure, and the two main mechanisms were revealed.
3. The first effects of corrosion were observed at the C_{of} - AZ31 interface at the time of 1 minute and progressed on the sample surface for up to 10 minutes, when the hydrophilic needle-like phase zone had been completely transformed into solid hydroxide and methane gas. Analysis of the progress of interface corrosion with time was conducted on cross sectioned samples and it confirmed that the type of corrosion progressed deep into the composite.
4. Corrosion products were revealed at the matrix surface of the C_{of} - AZ31 composite after 1 hour of exposure to the distilled water, which is a characteristic effect for magnesium alloys. Examination of the described composite corrosion confirmed differing corrosion resistance of the composite components, C_{of} and the AZ31 alloy, which are applied separately as biomaterials in medical practice. However, this study also revealed a gas emission effect at the interface, connected with the presence of hydrophilic phases in the as-manufactured material, and it points to magnesium alloys without aluminium as better candidates for a selectively corroded magnesium based composite biomaterial with carbon foam.

Acknowledgement

The study was carried out as a part of statutory research of the Institute of Materials Science at the Silesian University of Technology for 2018 (BK-221/RM0/2018).

REFERENCES

- [1] Hufenbach W., Andrich M., Langkamp A., Czulak A., Fabrication technology and material characterization of carbon fibre reinforced magnesium, *Journal of Materials Processing Technology* 2006, 175(1-3), 218-224.
- [2] Gryc A., Rzychoń T., Characterization of microstructure of WE43 magnesium matrix composites reinforced with carbon fibres, *Archives of Metallurgy and Materials* 2016, 61 (2B), 1075-1081.
- [3] Wang Y., Jiang L., Chen G., Lin X., Zhang S., Pei R., Wu G., Characterization of the reaction products and precipitates at the interface of carbon fiber reinforced magnesium-gadolinium composite, *Materials Characterization* 2016, 113, 232-238.
- [4] Olszówka-Myalska A., Myalski J., Magnesium alloy AZ31 - Short carbon fiber composite obtained by pressure die casting, *Solid State Phenomena* 2015, 229, 115-122.
- [5] Rashad M., Pan F., Lin D., Asif M., High temperature mechanical behavior of AZ61 magnesium alloy reinforced with graphene nanoplatelets, *Materials & Design* 2016, 89, 1242-1250.
- [6] Goh C.S., Wei J., Lee L.C., Gupta M., Simultaneous enhancement in strength and ductility by reinforcing magnesium with carbon nanotubes, *Materials Science and Engineering A* 2006, 423, 153-156.
- [7] Wong W.L.E., Gupta M., High performance lightweight magnesium nanocomposites for engineering and biomedical applications, *Nano World Journal* 2017, 2, 78-83.
- [8] Olszówka-Myalska A., Some physicochemical phenomena observed during fabrication of Mg-C cast composites, *Journal of Materials Engineering and Performance* 2016, 25 (8), 3091-3097.
- [9] Olszówka-Myalska A., Myalski J., Chrapoński J., Influence of casting procedure on microstructure and properties of Mg alloy-glassy carbon particle composite, *International Journal of Materials Research* 2015, 106(7), 741-749.
- [10] Chelliah N.M., Singh H., Surappa M.K., Correlation between microstructure and wear behavior of AZX915 Mg-alloy reinforced with 12 wt.% TiC particles by stir-casting process, *Journal of Magnesium and Alloys* 2016, 4 (4), 306-313.
- [11] Uozumi H., Kobayashi K., Nakanishi K., Matsunaga T., Shinozaki K., Sakamoto H., Tsukada T., Masuda C., Yoshida M., Fabrication process of carbon nanotube/light metal matrix composites by squeeze casting, *Materials Science and Engineering A* 2008, 495, 282-287.
- [12] Gawdzińska K., Nagolska D., Wojnar L., Effect of material and technological conditions on quality of metal matrix composite castings, *Solid State Phenomena* 2013, 197, 180-185.
- [13] Kremzer M., Dziekońska M., Sroka M., Tomiczek B., Abrasive wear of AlSi12-Al₂O₃ composite materials manufactured by pressure infiltration, *Archives of Metallurgy and Materials* 2016, 61(3), 1255-1260.
- [14] Myalski J., Hekner B., Posmyk A., Wpływ węglowej struktury szkieletowej na właściwości tribologiczne kompozytów z osnową aluminiową, *Tribologia* 2015, 5, 89-98.

- [15] San Marchi C., Kouzeli M., Rao R., Lewis J.A., Dunand D.C., Alumina-aluminum interpenetrating-phase composites with three-dimensional periodic architecture, *Scripta Materialia* 2003, 49, 861-866.
- [16] Dolata A.J., Centrifugal infiltration of porous ceramic preforms by the liquid alloy - theoretical background and experimental verification, *Archives of Metallurgy and Materials* 2016, 61 (1), 411-418.
- [17] Posmyk A., Myalski J., Composites including foam inserts designed for combustion engine cylinder liners, *Composites Theory and Practice* 2017, 17(1), 25-29.
- [18] Mehra D., Mahapatra M.M., Harsha S.P., Processing of RZ5-10wt%TiC in-situ magnesium matrix composite, *Journal of Magnesium and Alloys* 2018, 6(1), 100-105.
- [19] Olszówka-Myalska A., Myalski J., Godzierz M., Wrześniowski P., Magnesium matrix composite with open-celled carbon foam obtained by powder metallurgy, *Archives of Metallurgy and Materials* 2018, 63(2), 821-827.
- [20] Patent application No. P.422259, A. Olszówka-Myalska, J. Myalski, M. Godzierz.
- [21] Gu X.N., Zheng Y.F., Chen L.J., Influence of artificial biological fluid composition on the biocorrosion of potential orthopedic Mg-Ca, AZ31, AZ91 alloys, *Biomedical Materials* 2009, 4, 6 065011.
- [22] Johnston S., Shi Z., Atrens A., The influence of pH on the corrosion rate of high-purity Mg, AZ91 and ZE41 in bicarbonate buffered Hanks' solution, *Corrosion Science* 2015, 101, 182-192.
- [23] Zainal Abidin N.I., Rolfe B., Owen H., Malisano J., Martin D., Hofstetter J., Uggowitz P.J., Atrens A., The in vivo and in vitro corrosion of high-purity magnesium and magnesium alloys WZ21 and AZ91, *Corrosion Science* 2013, 75, 354-366.
- [24] Zhang E., Xu L., Yu G., In vivo evaluation of biodegradable magnesium alloy bone implant in the first 6 months implantation, *Journal of Biomedical Materials Research* 2009, 90A(3), 882-893.
- [25] Willbold E., Kaya A.A., Kaya R.A., Corrosion of magnesium alloy AZ31 screws is dependent on the implantation site. *Materials Science and Engineering: B* 2011, 176(20), 1835-1840.
- [26] Johnston S., Dargusch M., Atrens A., Building towards a standardized approach to biocorrosion studies: a review of factors influencing Mg corrosion in vitro pertinent to in vivo corrosion, *Science China Materials* 2018, 61(4), 475-500.
- [27] Li P., Zhou N., Qiu H., Maitz M. F., Wang J., Huang N., In vitro and in vivo cytocompatibility evaluation of biodegradable magnesium-based stents: a review, *Science China Materials* 2018, 61(4), 501-515.
- [28] Alijani S., Anvari A., Cycle numbers to failure for magnesium and its alloys in human body fluid, *Journal of Chemical Engineering and Materials Science* 2018, 9(1), 1-8.
- [29] Pec M.K., Reyes R., Sanchez E., Carballar D., Delgado A., Santamaria J., Arruebo M., Evora C., Reticulated vitreous carbon: a useful material for cell adhesion and tissue invasion, *European Cells and Materials* 2010, 20, 282-294.
- [30] Czarnecki J.S., Blackmore M., Jolivet S., Lafdi K., Tsonis P.A., Bone growth on reticulated vitreous carbon foam scaffolds and implementation of cellular automata modeling as a predictive tool, *Carbon* 2014, 79, 135-148.
- [31] Li Q., Turhan M.C., Rottmair C.A., Singer R.F., Virtanen S., Influence of MWCNT dispersion on corrosion behavior of their Mg composites, *Materials and Corrosion* 2012, 63, 384-387.
- [32] Bakkar A., Neubert V., Corrosion behaviour of carbon fibres/magnesium metal matrix composite and electrochemical response of its constituents, *Electrochimica Acta* 2009, 54, 1597-1606.
- [33] Godzierz M., Olszówka-Myalska A., Wrześniowski P., The interaction characteristics of liquid magnesium and selected magnesium alloys with open-celled glassy carbon foams, *Inżynieria Materiałowa/Materials Engineering* 2018, 222(2), 61-67.
- [34] Zhang D., Shen P., Shi L., Jiang Q., Wetting of B₄C, TiC and graphite substrates by molten Mg, *Materials Chemistry and Physics* 2011, 130, 665-671.
- [35] Shinozaki N., Morita J., Wasai K., Wetting of graphite by molten magnesium, *Journal of the Japan Institute of Light Metals* 2005, 55, 310-314.
- [36] Kielbus A., Precipitate processes in Mg-5Al magnesium alloy, *Solid State Phenomena* 2012, 191, 131-136.
- [37] Feldhoff A., Pippel E., Woltersdorf J., Carbon-fibre reinforced magnesium alloys: nanostructure and chemistry of interlayers and their effect on mechanical properties, *Journal of Microscopy* 1999, 196, 185-193.